Vol. 87 No. 2 pp. 454–466 ACTA GEOLOGICA SINICA (English Edition) Apr. 2013

Petrogenesis of the Langdu High–K Calc–Alkaline Intrusions in Yunnan Province: Constraints from Geochemistry and Sr–Nd Isotopes

REN Tao[1, *], ZHANG Xingchun[2], HAN Runsheng[1] and MA Meijuan[1]

1 *Faculty of Land and Resource Engineering, Kunming University of Science and Technology, Kunming 650093, Yunnan, China*

2 *State Key Laboratory of Ore Deposit Geochemistry, Institute of Geochemistry, Chinese Academy of Science, Guiyang 550002, Guizhou, China*

Abstract: The Langdu high–K calc–alkaline intrusions are located in the Zhongdian area, which is the southern part of the Yidun island arc. These intrusive rocks consist mainly of monzonite porphyry, granodiorite, and diorite porphyry. The K_2O content of majority of these rocks is greater than 3%, and, in the K_2O–SiO_2 diagram, all the samples fall into the high–K calc–alkaline to shoshonitic fields. They are enriched in light rare earth elements (LREEs) and depleted in heavy rare earth elements (HREEs; La_N/Yb_N = 14.3–21.2), and show slightly negative Eu anomalies (δEu = 0.77–1.00). These rocks have high K, Rb, Sr, and Ba contents; moderate to high enrichment of compatible elements (Cr = 36.7–79.9 ppm, Co = 9.6–16.4 ppm, and MgO = 2.2%–3.4%); low Nb, Ta, and Ti contents, and characteristic of low high field strength elements(HFSEs) versus incompatible elements ratios (Nb/Th = 0.75, Nb/La = 0.34) and incompatible elements ratios (Nb/U = 3.0 and Ce/Pb = 5.1, Ba/Rb = 12.0). These rocks exhibit restricted Sr and Nd isotopic compositions, with $(^{87}Sr/^{86}Sr)_i$ values ranging from 0.7044 to 0.7069 and $\varepsilon_{Nd}(t)$ values from -2.8 to -2.2. The Sr–Nd isotope systematic and specific trace element ratios suggest that Langdu high–K calc–alkaline intrusive rocks derived from a metasomatized mantle source. The unique geochemical feature of intrusive rocks can be modeled successfully using different members of a slightly enriched mantle, a slab–derived fluid, and terrigenous sediments. It can be inferred that the degree of partial melting and the presence of specific components are temporally related to the tectonic evolution of the Zhongdian island arc. Formation of these rocks can be explained by the various degrees of melting within an ascending region of the slightly enriched mantle, triggered by the subduction of the Garzê–Litang ocean, and an interaction between the slab–derived fluid and the terrigenous sediments.

Key words: high–K calc–alkaline intrusions, geochemistry, isotope, Zhongdian island arc

1 Introduction

High–K igneous rocks occur in most tectonic settings, including low–angle subduction environments (Njanko et al., 2006; Boztug et al., 2007), postorogenic settings (extension environments; Foley, 1992; Rottura et al., 1998; Benito et al., 1999; Neves et al., 2000; Acef et al., 2003; Njanko et al., 2006; Boztug et al., 2007; Oyhant et al., 2007; Putirka and Busby, 2007; Féménias et al., 2008), and intraplate or active continental margin environments (Morrison., 1980; Li et al., 2000, 2001). High–K calc–alkaline suites display a large compositional range, both in volcanic rocks (basalt, andesite, dacite, and rhyolite) and in their intrusions (gabbro, diorite, granodiorite, and granite). Studies of high–K calc–alkaline rocks are of special significance in the petrogenesis and regional tectonic evolution, in particular ancient tectonic reconstructions. As these rocks show a spatial and temporal association with mesothermal gold and porphyry copper–gold–molybdenum deposits. Therefore, their geochemical study not only has the potential economic geological significance, but also has become an important prospecting petrographic indicator.

Recently, a series of high–K calc–alkaline magmatic rocks has been identified in the eastern Tibetan plateau, located at the southern end of Yidun island arc belt, which is a part of the Sanjiang tectonomagmatic zone, SW

* Corresponding author. E-mail: rtao1982@126.com

China; this series include basalt, basaltic andesite, andesite, and intrusive rocks (Yang et al., 2002; Hou et al., 2003). Excluding the Bengge syenite, which is an ultrapotassic rock ($K_2O/Na_2O > 2$; Cao et al., 2007), all others plot in the potassic rocks field ($0.5 < K_2O/Na_2O < 2$). On the basis of the findings of previous works, this study has analyzed the major and trace elements and the Sr–Nd isotopes present in Langdu high–K calc–alkaline intrusions, to investigate the relationship between mafic and felsic magmatism; to track the source and, in particular, to assess metasomatism of hydrous fluid and subducted sediment in the mantle source; and to elucidate the nature of geodynamic processes.

2 Geological Settings

The Yidun island arc belt is a segment of the Tibetan–Himalayan giant orogenic system (Fig. 1a). The belt can be divided into Changtai, Xiangcheng, and Zhongdian island arcs from north to south (Hou et al., 2003). It was formed by the subduction of Garzê–Litang oceanic crust, superimposing with a continent–continent or arc–continent collision and the postorogenic extension (Hou et al., 2001, 2004; Yang et al., 2002; Wan and Zhu, 2011; Xiao et al., 2004). Various magmatisms have occurred in various tectonic setting.

The Zhongdian island arc is located at the southern part of the Yidun island arc belt (Fig. 1a). It is constrained by the Garzê–Litang suture zone on its east and south sides and by the NNW–trending Xiangcheng fault on its west side; the south side extends to the Tuguan village (Fig. 1a; Yang et al., 2002; Zeng et al., 2004). The development of this volcanic arc experienced three epochs: subduction, arc–continent collision (intracontinental convergence) and postorogenic extension (Yang et al., 2002; Hou et al., 2003).The volcanic rocks that outcrop in the Zhongdian region include those of the late Triassic Qugasi (Fig. 1b; Carnian) and Tumugou (late Carnian to early Norian) Formations. The Qugasi Formation consists of three members: the lower member is composed of massive basalt and andesitic–basaltic volcanic breccia; second member is composed of basalt; and upper member consists dominantly of altered basaltic tuff and basaltic volcanic breccia. The Tumugou Formation consists of acidic volcanic rocks (Fig. 1b). These acidic volcanic rocks are significantly more active than the basalts. In petrography, the rocks are classified as andesite, andesitic tuff, andesitic breccia, and dacitic tuff. All these rocks belong to the high–K calc–alkaline series.

In this region, Indosinian intrusions are widely exposed (Fig. 1b); representative intrusions, consisting of quartz diorite porphyry, quartz monzonite porphyry, granodiorite porphyry, and dacite porphyry, include Pulang, Xuejiping, Langdu, Chundu, Hongshan, Songnuo, etc. These intrusions are closely related to copper–polymetallic mineralization, and have formed a number of huge economic porphyry copper and skarn copper deposits, such as Pulang, Xuejiping, and Chundu porphyry copper deposits; Langdu and Hongshan skarn copper deposits, etc. Yanshanian intrusive rocks are mainly distributed in the northern part of the region (Fig. 1b). Representative intrusions are Relin and Xiuwacu porphyritic biotite monzonitic granites. The total rock Rb–Sr isochron ages of the Relin and Xiuwacu intrusions are estimated to be 80.4 and 88 ± 3 Ma (Hou et al., 2003), respectively. Yanshanian granites could have formed in a postcollisional environment (Hou et al., 2003). Himalayan magmatism, mostly located on the edge of the original Yaza porphyry (Indosinian), is dacite porphyry. K–Ar dating of hornblende has yielded ages of 53.02 ± 1.06 Ma (Zeng et al., 2004).

Many hypabyssal to ultrahypabyssal intrusive rocks are exposed in the Langdu area, with an outcrop area of about 0.9 km^2. These intrusions developed in the upper Triassic Qugasi Formation and are controlled by the northwest–trending Wodicuo and northeast–trending Bidu fractures. They are classified as monzonite porphyry, quartz diorite porphyry, and granodiorite porphyry. Phenocryst minerals include plagioclase, K–feldspar, hornblende, biotite, and quartz, and accessory minerals contain titanite, apatite, and zircon. In this study, fresh rocks were collected from the Langdu mine for sample analysis.

3 Analytical Methods

Major elements were determined by a PANalytical Axiosadvance X–ray fluorescence spectrometer at the State Key Laboratory of Ore Deposit Geochemistry (SKLODG), Institute of Geochemistry, Chinese Academy of Sciences, using fused lithium–tetraborate glass pellets. Trace elements were analyzed using a Perkin–Elmer Sciex ELAN DRC ICP–MS at the SKLODG. The powdered samples (50 mg) were dissolved in high–pressure Teflon bombs using a mixture of HF and HNO_3 acids, for 48 h at ~190°C (Qi et al., 2000). Rh was used as an internal standard to monitor signal drift during counting. The international standards such as GBPG–1, OU–6 were used for analysis. The analytical precision is generally better than 5% for trace elements. Samples for Sr and Nd isotopic analysis were dissolved in Teflon bombs with $HF+HNO_3$ acid, and separated by conventional cation–exchange techniques. The isotopic measurements were performed on a Thermo Fisher TRITON at the SKLODG. The mass fractionation corrections for Sr and Nd isotopic

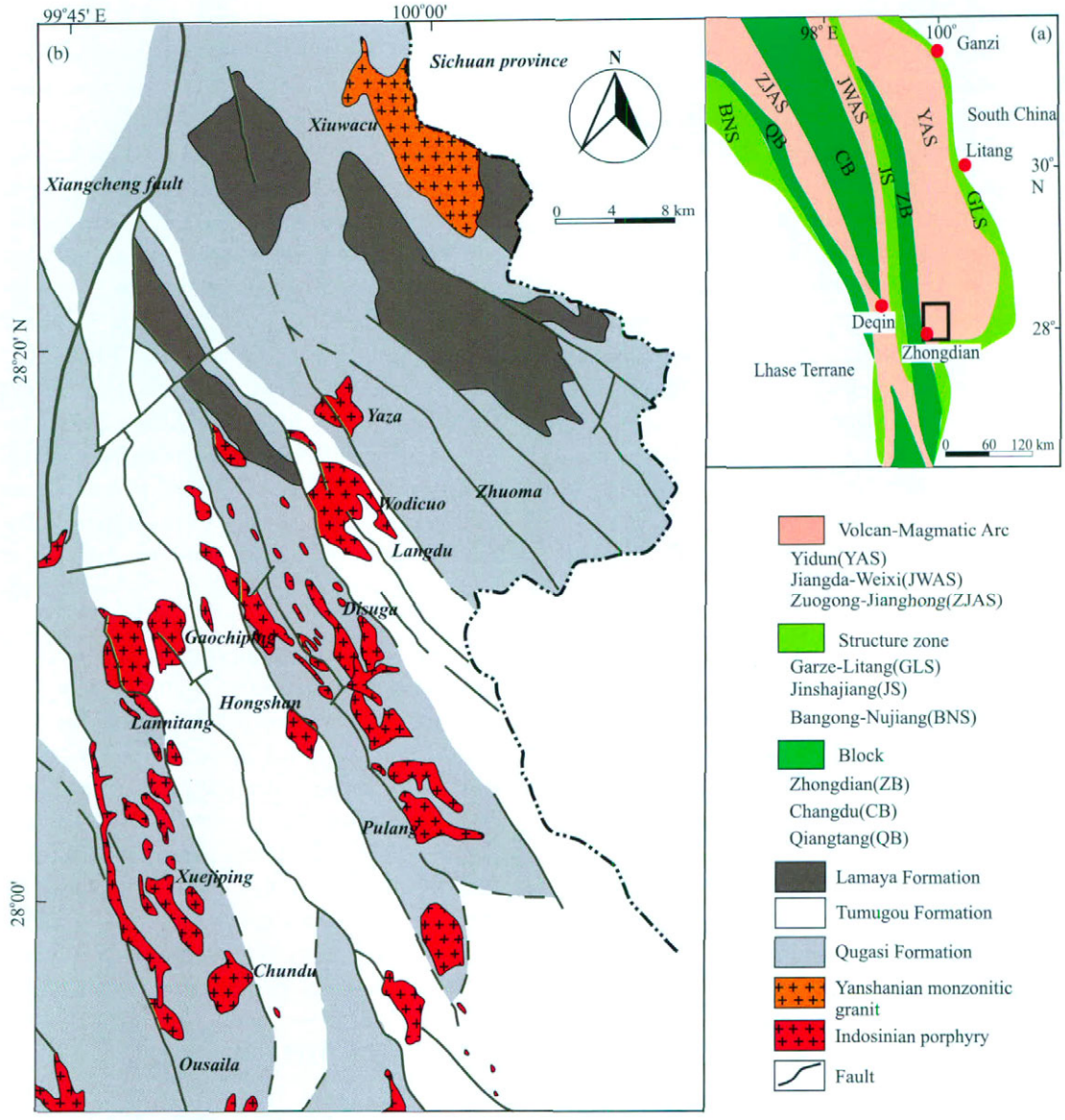

Fig. 1. Simplified geological map showing tectonic framework of the Sanjiang Tethys (Fig. 1a; after Mo et al. 1993). Sketch geological map of zhongdian area (Fig. 1b; after Zeng et al. 2002).

ratios were carried out based on $^{86}Sr/^{88}Sr$=0.1194 and $^{146}Nd/^{144}Nd$=0.7219, respectively. As determined during this study, the $^{87}Sr/^{86}Sr$ values of the NBS987 standard and $^{143}Nd/^{144}Nd$ ratios of the BCR–2 and JNdi–1 standards were 0.710250±7 (2σ), 0.512612±8 (2σ), and 0.512104±5 (2σ), respectively.

4 Results

4.1 Major and trace elements

The results of the analysis of major and trace elements in representative samples are listed in Table 1. These rocks span a narrow range of SiO_2 content (60.8%–63.6%), belong to middle–acidic rocks, and are high in total alkalis ($K_2O + Na_2O$ = 6.53%–8.22%). In the Middlemost (1994) rocks classification diagram, all samples fall into the monzonite and quartz monzonite fields, defined as the calc –alkaline series (Fig. 2a). The Al_2O_3 content of these rocks vary from 13.98% to 15.25%. In the ANK–ACNK diagram, these plot in the metaluminous region (Fig. 2b). In the K_2O–SiO_2 diagram, the rocks fall into the high–K calc–alkaline and shoshonitic rock fields (Fig. 2c). They exhibit high K_2O contents (K_2O/Na_2O =1.03–1.79) and are typical potassium series rocks, rather than belonging to the ultrapotassic series (Fig. 2d). Harker diagrams (Fig. 3) show the variations of representative major elements as a function of SiO_2 contents in the rocks. With an increase in the silica content, contents of CaO, TiO_2, P_2O_5, Fe_2O_3, and MgO decrease; content of K_2O increases; and content of Na_2O shows an unclear trend (Fig. 3).

Selected elements are plotted against SiO_2 contents in Fig. 4. Concentrations of Sr and Ba decrease (Figs. 4b,

Table 1 Major (%) and trace (ppm) elements data for the Langdu high−K calc−alkaline intrusions

Sample No.	LD0717	LD0733	LD0734	LD0735	LD0737	LD0738	LD0743	LD0744	LD0745	LD0747	LD0801	LD0802	LD0803	LD0810
SiO_2	62.83	60.91	61.36	60.84	60.94	61.04	61.14	61.56	62.10	61.67	61.73	61.16	62.58	62.36
Al_2O_3	14.88	15.25	14.84	14.87	14.68	15.01	14.70	14.65	13.98	14.64	14.75	15.40	14.46	14.78
Fe_2O_3	4.34	5.57	5.20	5.28	5.44	5.11	4.89	5.00	4.46	5.01	4.80	4.45	4.39	4.49
MgO	2.42	3.41	3.14	3.28	3.28	3.16	2.52	2.73	2.50	2.80	2.86	2.53	2.22	2.42
CaO	4.44	5.34	5.44	5.25	4.99	5.28	4.11	4.31	4.04	4.15	4.34	3.86	3.94	3.99
Na_2O	3.36	3.18	3.28	3.22	3.06	3.16	3.24	3.35	3.66	3.22	3.68	3.26	3.00	2.83
K_2O	4.60	4.20	3.55	3.31	4.12	4.08	4.91	4.42	3.81	4.36	4.54	4.93	4.50	5.08
MnO	0.07	0.08	0.07	0.10	0.11	0.07	0.08	0.11	0.11	0.12	0.09	0.06	0.05	0.07
P_2O_5	0.33	0.38	0.37	0.37	0.37	0.37	0.35	0.34	0.35	0.34	0.36	0.34	0.37	0.33
TiO_2	0.55	0.63	0.64	0.64	0.62	0.63	0.58	0.58	0.60	0.58	0.60	0.56	0.57	0.56
LOI	2.42	0.99	2.41	1.75	1.41	1.16	3.23	2.59	3.64	2.02	2.51	3.90	4.55	3.26
Total	100.24	99.94	100.29	98.91	99.03	99.07	99.74	99.63	99.24	98.90	100.25	100.45	100.63	100.16
Sc	14.4	16.0	16.0	15.3	14.3	16.2	12.7	13.2	14.0	12.3	15.0	14.0	13.2	7.4
V	119	132	131	143	138	131	112	125	99.4	121	113	112	103	113
Cr	51.5	66.7	63.5	63.3	66.3	79.9	55.8	49.4	50.1	48.8	44.0	62.8	36.7	56.7
Co	15.2	15.3	14.0	15.2	16.4	14.5	10.7	13.5	9.56	13.3	12.9	12.6	14.1	13.3
Rb	211	125	107	113	174	122	173	129	108	123	118	175	73.7	131
Sr	659	858	877	941	719	874	735	739	625	829	881	820	753	896
Y	15.1	16.1	16.2	16.5	16.2	15.9	15.0	16.1	14.1	15.4	17.4	15.6	9.69	15.8
Zr	172	149	138	110	169	118	106	169	131	155	182	161	177	116
Nb	10.3	9.71	10.40	10.12	11.81	9.80	10.1	10.6	10.4	10.3	10.9	10.8	9.85	10.0
Ba	1350	1830	1500	1498	1095	1770	1580	1701	1168	1788	1433	1346	1400	5160
Hf	4.07	3.88	3.75	2.97	2.79	3.25	2.97	4.28	3.26	3.77	2.69	2.52	4.43	2.92
Ta	0.75	0.69	0.77	0.83	0.64	0.71	0.75	0.84	0.86	0.80	0.50	0.54	0.55	0.75
Pb	5.08	8.90	10.3	21.4	6.62	11.3	13.6	34.5	14.7	26.9	12.0	8.69	9.96	12.9
Th	17.0	16.2	17.3	14.8	12.4	16.6	16.0	13.8	16.5	15.3	10.4	12.5	8.95	14.0
U	3.27	3.50	3.75	3.84	3.17	3.53	3.29	4.05	3.70	4.00	2.54	2.91	3.82	3.65
La	34.6	36.6	34.7	33.4	23.5	39.0	35.2	30.3	32.9	30.9	26.0	24.9	24.3	31.6
Ce	57.7	62.8	60.2	60.7	46.5	66.7	60.3	55.4	59.5	56.4	50.2	48.6	47.7	58.7
Pr	6.41	7.17	6.77	7.05	4.60	7.51	6.71	6.29	6.57	6.32	4.96	4.71	5.21	6.69
Nd	23.1	26.4	25.6	26.2	17.1	27.9	25.1	23.3	23.9	23.4	17.9	17.5	19.1	24.6
Sm	4.51	5.00	5.01	5.06	3.23	5.43	4.72	4.47	4.60	4.43	3.60	3.17	3.78	4.79
Eu	1.26	1.34	1.30	1.42	0.77	1.36	1.25	1.27	1.01	1.20	0.85	0.76	1.06	1.10
Gd	3.07	3.84	3.52	4.15	2.64	3.59	3.13	4.03	3.63	3.88	2.71	2.76	2.45	4.25
Tb	0.54	0.63	0.64	0.60	0.39	0.67	0.57	0.53	0.51	0.57	0.40	0.37	0.47	0.57
Dy	2.51	2.92	2.95	3.22	1.81	2.92	2.67	3.02	2.67	2.86	1.84	1.81	2.20	3.00
Ho	0.52	0.58	0.57	0.58	0.36	0.57	0.55	0.55	0.49	0.55	0.35	0.35	0.46	0.52
Er	1.36	1.59	1.59	1.61	1.00	1.55	1.44	1.54	1.26	1.49	1.00	0.94	1.25	1.52
Tm	0.18	0.23	0.21	0.21	0.14	0.21	0.19	0.21	0.18	0.20	0.12	0.12	0.16	0.20
Yb	1.19	1.43	1.44	1.37	0.93	1.34	1.26	1.43	1.20	1.44	0.83	0.83	1.12	1.35
Lu	0.18	0.21	0.21	0.23	0.14	0.20	0.19	0.22	0.16	0.21	0.13	0.12	0.17	0.21

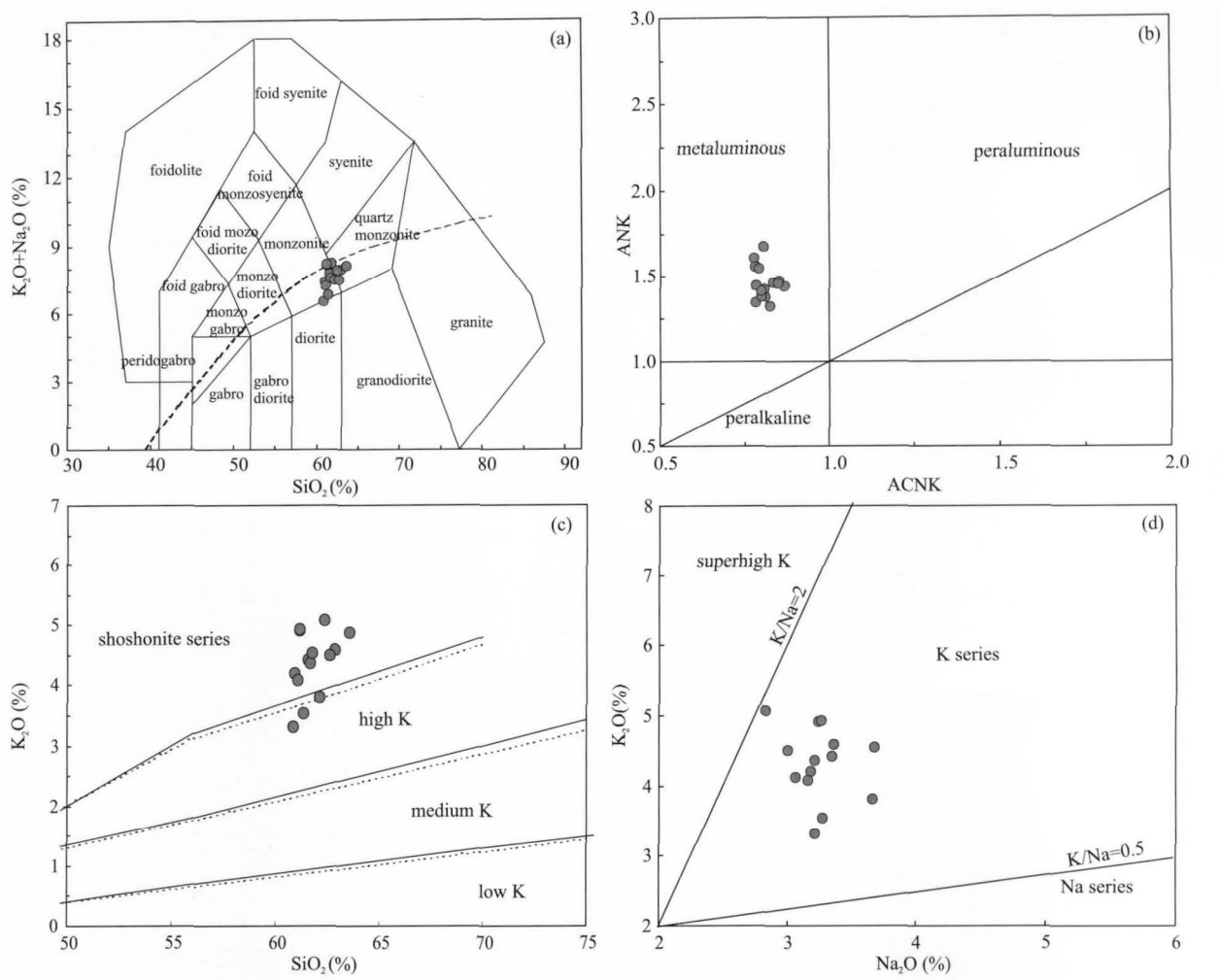

Fig. 2. (a) Rocks of the Langdu high–K calc–alkaline intrusions plotted on the Middlemost (1994) classification diagram; (b) Chemical composition of the Langdu high–K calc–alkaline intrusions in terms of alumina saturation diagram; (c) SiO_2 vs. K_2O diagram for Langdu high–K calc–alkaline intrusions; (d) N_2O vs. K_2O diagram for Langdu high–K calc–alkaline intrusions.

4c), whereas those of Rb and Zr increase with increasing SiO_2 content (Figs. 4a, 4d). All samples have high contents of total rare earth elements (REEs). Chondrite–normalized REE profiles of Langdu high–K calc–alkaline intrusions (Fig. 5a) show that these are enriched in light REEs (LREEs) and depleted in heavy REEs (HREEs; La_N/Yb_N = 14.3–21.2). These rocks have a weakly negative Eu anomaly (the δEu = 0.77–1.00). In primitive mantle–normalized spider diagrams (Fig. 5b), intrusive rocks exhibit high concentrations of large–ion lithophile elements (LILEs), Sr, and Pb, whereas low concentrations of Nb, Ta, and Ti. The characteristics and distribution patterns of these trace elements are similar to those of the regional intrusions of Pulang, Xuejiping, and Chundu porphyry, and also of the K–rich igneous rocks worldwide (Hou et al., 2003; Boztug et al., 2007).

4.2 Sr–Nd isotopic compositions

The Sr and Nd isotopic compositions of samples from the Langdu high–K calc–alkaline intrusions are presented in Table 2. Initial Sr–Nd isotope ratios are calculated at t = 216 Ma (Zeng et al., 2004). These rocks show restricted Sr and Nd isotopic compositions, with initial values of $^{87}Sr/^{86}Sr$ varying from 0.7044 to 0.7069 and of $^{143}Nd/^{144}Nd$ from 0.512214 to 0.512249. Initial ε_{Nd} values are all slightly negative and range from –2.8 to –2.2, indicating that the magma source has a homogeneously isotopic composition (Fig. 6). In the Sr versus Nd isotopic composition diagram (Fig. 7), isotopic values of the samples are similar to those of Western Australia, Ullung–do, and Batu Tara potassium–rich igneous rocks; andesites in Tumugou Formation, and Pulang and Xuejiping porphyries in the region (Fig. 7).

5 Discussions and Conclusions

5.1 Magma sources

Numerous studies conducted earlier suggest that there

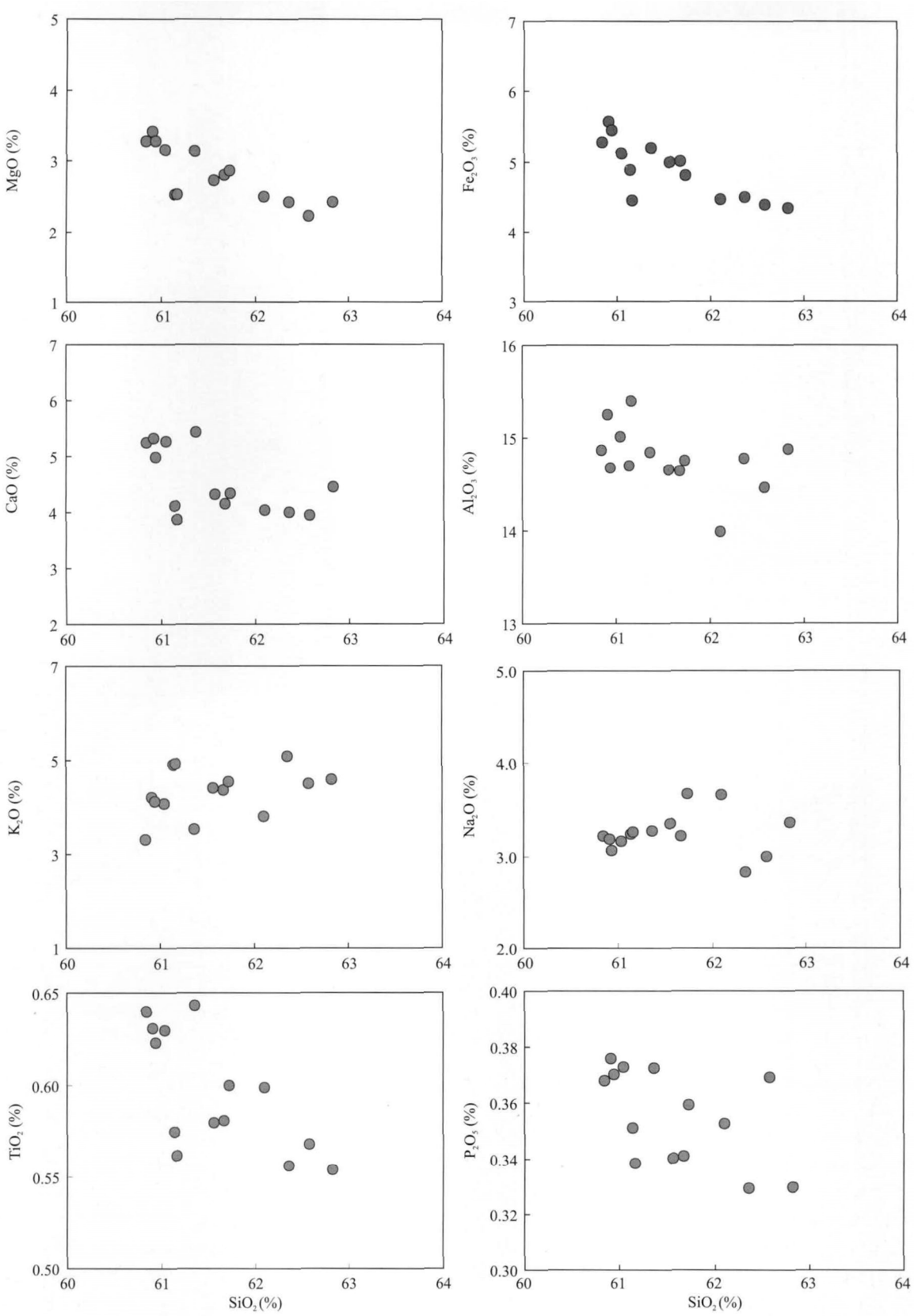

Fig. 3. Selected variation diagrams of major element oxides and silica for the samples from Langdu high–K calc–alkaline intrusions.

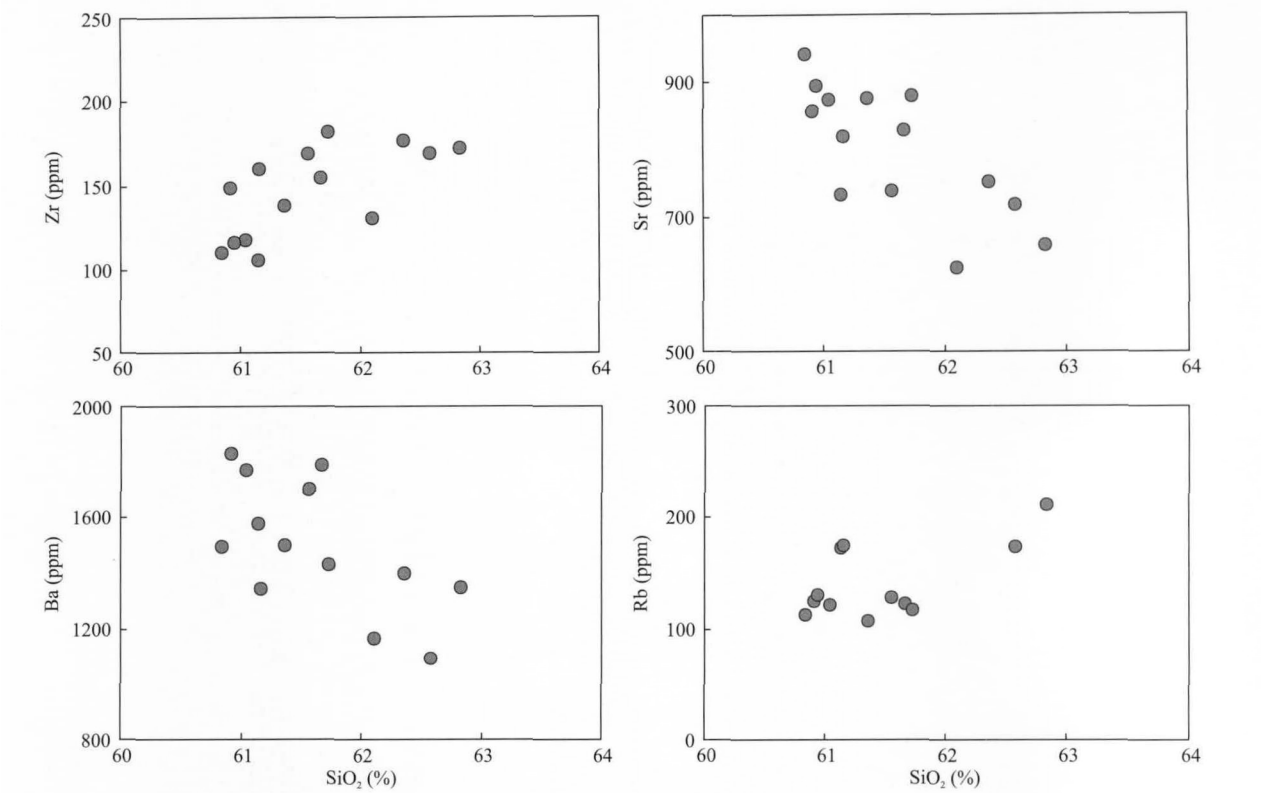

Fig. 4. Selected variation diagrams of trace elements and silica for the Langdu high–K calc–alkaline intrusions.

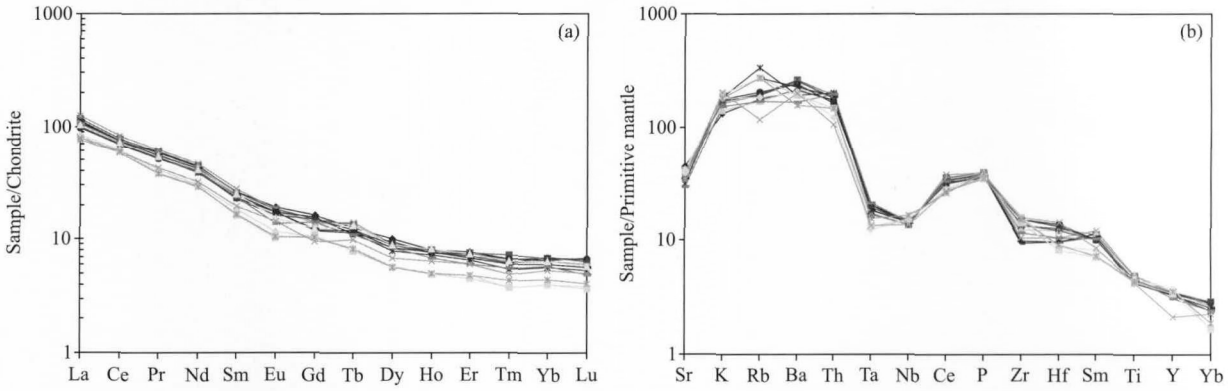

Fig. 5. (a) Chondrite–normalized REE diagrams and (b) Primitive mantle–normalized trace element distribution spidergrams for the Langdu high–K calc–alkaline intrusions. The normalization values are from Sun and McDonough (1989).

are three material sources and genetic models for potassic igneous rocks: (1) Those derived from LILE– and LREE–rich mantle source, such as Roccamonfia, central Italy, Boreborema, and Iran potassium–rich rocks, which are considered mainly to be related to sediment contamination (especially oceanic sediments; Foley, 1992; Rottura et al., 1998; Benito et al., 1999; Neves et al., 2000; Acef et al., 2003; Njanko et al., 2006; Boztug et al., 2007; Oyhant et al., 2007; Féménias et al., 2008). (2) Those formed by a low–degree partial melting of asthenospheric mantle, followed by fractional crystallization, such as Sierra Nevada potassium–rich volcanic rocks (Putirka and Busby, 2007). (3) Those formed by partial melting of asthenospheric mantle and interaction with overlying lithospheric mantle, such as Yuexi–Guidong high–K intrusive rocks (Li et al., 2000, 2001).

5.1.1 Mantle source components

Hou et al. (2003) suggested that basalt occurring in Qugasi Formation should be oceanic or continental transition rifting environment volcanic rocks, similar to the Changtai former island arc basalt. The basalt has a high concentration of LILEs, and a slightly high concentration of high field strength elements (HFSEs). In the Zr–Ti and TiO_2–FeO*/MgO tectonic environment discrimination diagram, majority of the rocks fall into the MORB region, while in the Zr/Nb–$(La/Sm)_N$ diagram, the rocks fall into the N–MORB and E–MORB mixing line, reflecting the

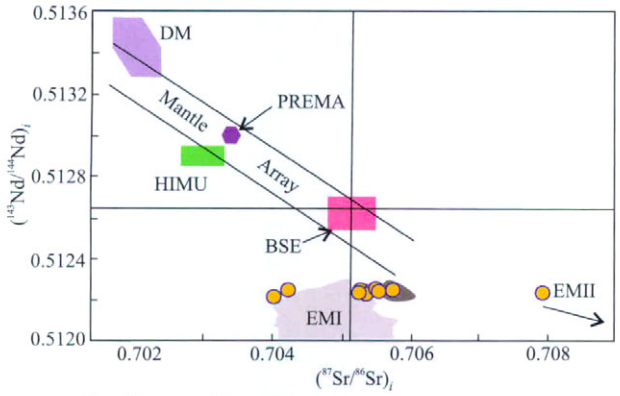

Fig. 6. $^{87}Sr/^{86}Sr$ vs. $^{143}Nd/^{144}Nd$ diagram for Langdu high–K calc–alkaline intrusions (DM, HIMU, PREMA, BSE, EMI and EM II are from Zindler et al. (1986)).

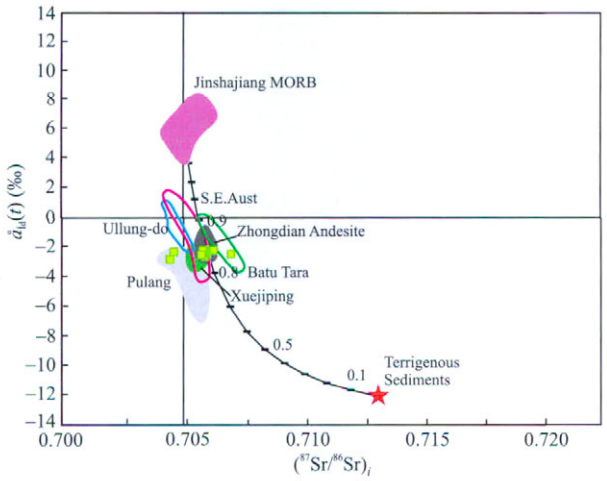

Fig. 7. $^{87}Sr/^{86}Sr$ vs. $\varepsilon_{Nd}(t)$ diagram for Langdu high–K calc–alkaline intrusions. The Jinshajiang ophiolite field is from Xu and Castillob (2004). The compotion of average terrigenous sediments is from Lan et al. (1990). The isotopic composition of Xuejiping and Pulang are from Leng et al. (2009) and Wang et al. (2008) respectively. The data of Ullung–do, S.E.Aust and Batu Tara are from Nelson (1992).

characteristics of a low–degree enriched mantle. E–MORB can be formed by assimilation of crustal material or fluid metasomatism (Hou et al., 2003; Li et al., 2012).

The Langdu high–K calc–alkaline intrusions have high contents of K_2O; high LREEs and LILEs; a moderate content of MgO; low contents of Al_2O_3, CaO, and Fe_2O_3; low HREEs and HFSEs; and slightly low Nd and high Sr isotopic values, suggesting that the magma could have been derived from EMI (Fig. 6; With et al., 1982; Zindler et al., 1986). EMI has been defined by Hart (1984) and its genesis is still disputed. According to Palacz et al. (1986), the delaminated bottom of the lithospheric mantle is the ideal source of EMI; as Hart (1988) assessed, EMI is derived from the core–mantle boundary; and as proposed by Weaver et al. (1986), EMI originates from the mix of subduction sediments and oceanic island basalts. Majority of researchers believed that EMI is the small volume of potassium and volatile rich melt in asthenosphere, or slab–derived fluid metasomatized lithospheric mantle (Calvin et al., 2003).

5.1.2 Subduction components

Langdu high–K calc–alkaline intrusions exhibit moderate to high contents of compatible elements (Cr = 36.7–79.9 ppm, Co = 9.6 –16.4 ppm) and MgO (2.2%–3.4%), suggesting a mantle origin, whereas high contents of the LILEs and LREEs and slightly negative ε_{Nd} values reflect a crustal source material. Yang et al. (2002) and Hou et al. (2003) suggested that andesites in the Zhongdian area were derived through partial melting of the metasomatized mantle. The two–stage Nd model ages (depleted mantle), which range from 1171 to 1226 Ma (Table 2), also supported this view. Wang et al. (2008) suggested that the Nd model ages may represent the mixing of the ancient crust components or the mantle material.

Based on the above discussions, and considering that the Jinsha River ophiolites belong to the Sanjiang tectonic zone (Sanjiang igneous rocks have a similar mantle source) located in the west of Yidun island arc and average global terrigenous sediments represent the end members, mixing calculations based on their Sr–Nd isotopic values

Table 2 Sr and Nd isotopic data for Langdu high–K calc–alkaline intrusions

Sample No.	Rb (ppm)	Sr (ppm)	$^{87}Rb/^{86}Sr$	$^{87}Sr/^{86}Sr$	2σ	$(^{87}Sr/^{86}Sr)_i$	Nd (ppm)	Sm (ppm)	$^{147}Sm/^{144}Nd$	$^{143}Nd/^{143}Nd$	2σ	$(^{147}Sm/^{144}Nd)_i$	$\varepsilon_{Nd}(t)$	T_{DM2} (Ma)
LD-0733	125	858	0.4216	0.707102	±6	0.705653	26.4	5.00	0.1144	0.512411	±1	0.512240	−2.15	1171
LD-0734	107	877	0.3530	0.707130	±5	0.705590	25.6	5.01	0.1182	0.512412	±1	0.512246	−2.24	1178
LD-0738	122	874	0.4039	0.707092	±5	0.705667	27.9	5.43	0.1176	0.512405	±2	0.512224	−2.36	1188
LD-0743	173	735	0.6811	0.707679	±5	0.704442	25.1	4.72	0.1136	0.512393	±1	0.512214	−2.48	1198
LD-0801	117	881	0.3865	0.706845	±4	0.706862	17.9	3.60	0.1214	0.512412	±1	0.512229	−2.32	1185
LD-0802	175	820	0.6173	0.707494	±4	0.704631	17.5	3.17	0.1091	0.512401	±1	0.512242	−2.20	1175
LD-0803	173	719	0.6999	0.707826	±3	0.705801	17.1	3.23	0.1140	0.512386	±2	0.512249	−2.63	1210
LD-0804	158	363	1.2595	0.708328	±4	0.706041	24.6	4.88	0.1199	0.512384	±1	0.512244	−2.83	1226
LD-0810	73.7	753	0.6675	0.708921	±5	0.705846	19.1	3.78	0.1196	0.512399	±1	0.512238	−2.53	1202
LD-0817	211	659	0.9265	0.707489	±5	0.705578	23.1	4.51	0.1180	0.512409	±1	0.512232	−2.29	1182

show that 15% terrigenous sediments need to be added to the enriched mantle to yield a possible source for Langdu high–K calc–alkaline intrusions (Fig. 7).

However, the high Nd and Sr isotopic values, and characteristic incompatible element ratios (Nb/U = 3.0 and Ce/Pb = 5.1, Ba/Rb = 12.0) and ratios of HFSEs versus incompatible elements (Nb/Th = 0.75, Nb/La = 0.34) cannot be explained by sediment contamination. Wang et al. (2008) suggested that a new end member of nonmagmatic composition is required. The slab–derived fluid effect is clearly shown by plots of Ba/Rb versus Nb/La and Ce/Pb versus Th/La (Fig. 8). In addition, mineral–aqueous fluid experiments and previous studies of high–K calc–alkaline rocks (Benito, 1999; Oyhantcabal, 2007) also suggest that the enrichment agent may be the subduction zone fluid.

The average chemical compositions of global continental sediments were chosen to represent the chemical compositions of Garzê–Litang oceanic subducted terrigenous sediments. Chemical compositions of the slab–derived fluid were defined by Tatsumi and Kogiso (1997) and Ayers (1998). Using E–MORB as a starting material representing local enriched mantle source. As per the calculation results shown in Fig. 9, all rocks plot along a mixing trend between the terrigenous sediments and the slab–derived fluid. A terrigenous sediment dominated metasomatism, coupled with about 20–30% slab–derived fluid contribution from average terrigenous sediment. Based on experimental studies, Roberts (1993) suggested that the most appropriate source for high–K calc–alkaline rocks is a hydrous, calc–alkaline to high–K calc–alkaline, andesitic to basaltic andesitic melt, which is consistent with the calculations. Homogeneous Sr–Nd isotopic composition; relatively low contents of Na, Al, V, and Sc; and relatively high contents of Ni and Cr indicate that the contamination of crustal materials took place prior to partial melting (Conticellia, 1992).

In summary, the petrological and geochemical data imply that at least three end members contributed to the genesis of Langdu high–K calc–alkaline intrusions. The source evolution could experience two processes. In the first process, slab–derived fluids metasomatized the low–degree enriched mantle. The enriched mantle with relatively low contents of La, Rb, Zr, Ce, Nd, Sm, Eu, Tb, Hf, Ta, U, and Th and low Sr–Nd isotopic values transformed into a metasomatized mantle with high contents of LILEs and LREEs, and Sr–Nd isotopes. In the second process, the metasomatized mantle interacted with

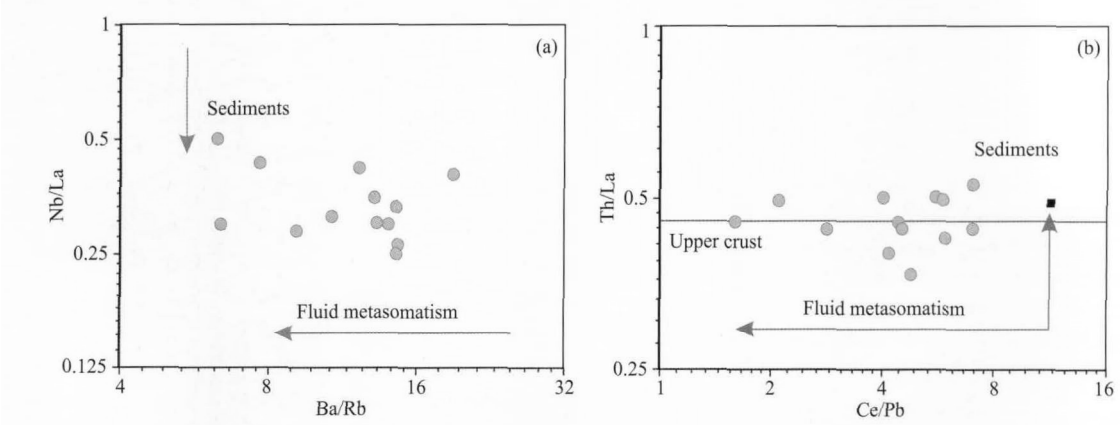

Fig. 8. (a) Nb/La vs. Ba/Rb diagram and (b) Th/La vs. Ce/Pb diagram for Langdu high–K calc–alkaline intrusions. Ratios of Th/La and Ce/Pb are from Plank (2005) and Wang et al. (2004) respectively.

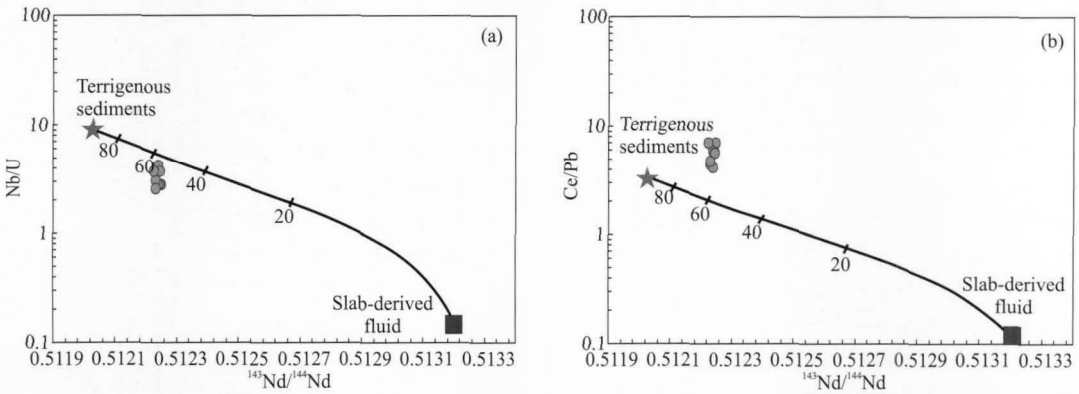

Fig. 9. (a) Nb/U vs. $^{143}Nd/^{144}Nd$ and (b) Ce/Pb vs. $^{143}Nd/^{144}Nd$ diagrams for Langdu high–K calc–alkaline intrusions. Data for slab–derived fluid is from Tatsumi and Kogiso (1997) and sediment is from Lan et al. (1990).

the terrigenous sediment, resulting in a source more enriched in Sr and Nd isotopes. It has been noted that the two processes should be simultaneous in time.

5.2 Fractional crystallization

In the $\varepsilon_{Nd}(t)$ versus Nd diagram (Fig. 10a), the Langdu high–K calc–alkaline intrusions exhibit fractional crystallization. With increasing silica content, contents of CaO, TiO_2, P_2O_5, Fe_2O_3, and MgO decrease, suggesting igneous fractionation involving pyroxene, apatite, and ilmenite. Contents of Al_2O_3 decrease, of K_2O increase, and of Na_2O do not show any obvious change with an increase in the SiO_2 content, indicating that there is no significant feldspar fractionation. In the REE chondrite–normalized diagrams (Fig. 5a), the pattern shows a relatively flat middle REE profile, which can readily be attributed to an amphibole–free fractionation; a stable Y content with an increase in the SiO_2 content (Fig. 10b) also reflects an amphibole–free fractionation. With an increase in the SiO_2 content, Sr and Ba contents decrease (Fig. 4), Rb content is not changed, and slightly negative Eu anomalies are obtained (δEu = 0.77–1.0), which can be explained by the fractionation of a small amount of potassium feldspar.

5.3 Petrogenetic model

The Langdu high–K calc–alkaline intrusions exhibit unobvious negative Eu anomalies, and all samples show positive Sr anomalies (Fig. 5b), reflecting the fact that the magma cannot be derived from mantle–derived primary basaltic magma and that magma sources are plagioclase free or plagioclase residues cannot be formed. HREEs are enriched in garnet under high pressure (Hanson, 1978; Evans et al., 1993); the Langdu high–K calc–alkaline intrusions, although strongly depleted in HREEs, usually represent the magma source that is garnet rich or close to the garnet stability conditions. Experimental petrology studies have shown that the garnet stability pressure normally varies from 1.0 to 1.5 GPa. In general, garnet is not the residual component of the acidic magma; however as the pressure increases, the amount of garnet gradually increases and that of plagioclase decreases or even disappears from the residue (Montel et al., 1997; Litvinovsky et al., 2000). According to the preceding discussion, it can be speculated that the original magma of Langdu high–K calc–alkaline intrusions melted under the high–pressure condition, which is greater than the garnet stability boundary (P = 1.0–1.5 GPa) and consistent with the pressure at a depth of at least 35 km (>1.0 GPa).

The Langdu high–K calc–alkaline intrusions show high Sr concentration, high Sr/Y and La/Yb ratios, low Y and Yb concentrations, and slightly negative Eu anomalies, indicating that the tectonic setting is of orogenic or subduction type. In the TiO_2/Al_2O_3–Zr/Al_2O_3 and Zr/TiO_2–Ce/P_2O_5 joint tectonic discrimination diagram (Fig. 11), all the rocks plot in the range of the continental margin arc fields, providing further evidence in favor of the fact that the Zhongdian island arc has been formed at an active continental margin (Hou et al., 2003).

5.4 Geodynamic model

Previous studies suggest that the Garzê–Litang ocean basin opened during the Late Permian to Early Triassic (Fig. 12a; before 237 Ma; Mo et al., 1993), the average expansion rate being 0.85 cm/year, leading to the final width of 476 km (Mo et al., 1993). Hou et al. (2003) pointed out that the basalt in the Qugasi Formation should belong to the oceanic or continental transition rifting environment volcanic rocks, which are similar to the basalt of Changtai island arc. K–Ar dating of the Changtai basalt has yielded ages of 231 Ma (Hou et al., 2003). Now, the general agreement is that subduction of the Garzê–Litang ocean basin began at 237 Ma, along with the abatement of the oceanic crust under the Zhongza microcontinental block (Fig. 12a). Increases in temperature and pressure, due to descending of the oceanic crust, induced metamorphism and dehydration of

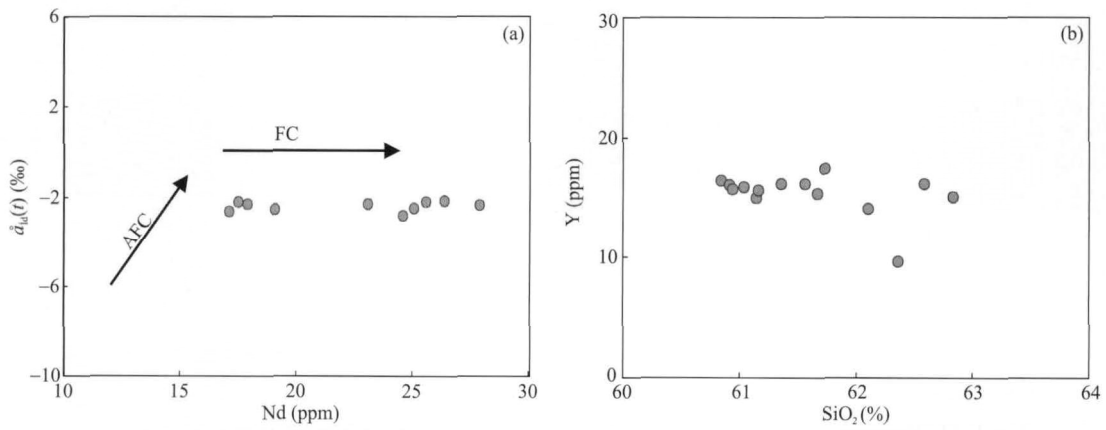

Fig. 10. $\varepsilon_{Nd}(t)$ vs. Nd and Y vs. SiO_2 diagrams for Langdu high–K calc–alkaline intrusions.

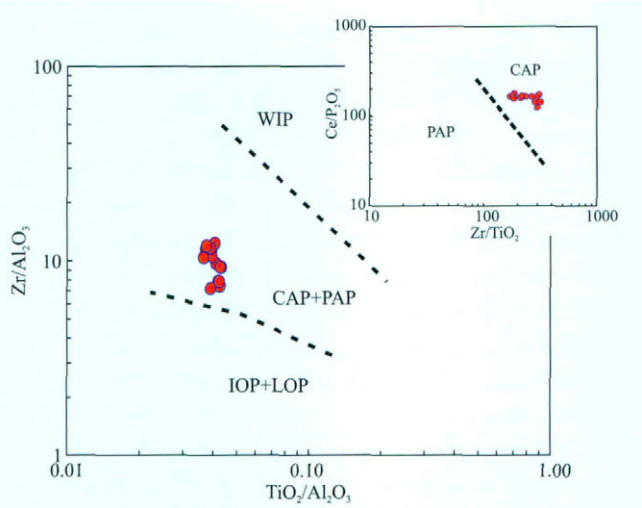

Fig. 11. TiO_2/Al_2O_3 vs. Zr/Al_2O_3 and Zr/TiO_2 vs. Ce/P_2O_5 diagrams for Langdu high–K calc–alkaline intrusions.

subduction slab and terrigenous sediments. The slab–derived fluids that were released had high concentrations of LREEs and LILEs, and a low content of HFSEs. The andesitic and basaltic andesite melt ejected and emplaced in the Zhongdian area to form, respectively, the Tumugou andesite and the high–K calc–alkaline intrusive rocks, originated by partial melting of the mantle wedge, which was metasomatized by the slab–derived fluid and terrigenous sediments. A zircon SHRIMP dating yields an age of 220 Ma for the andesite (Leng et al., 2009). Island arc and back–arc basin occurred along the subduction direction, forming a complete trench–arc–basin system (Fig. 12b; Hou et al., 2004).

High–K calc–alkaline intrusive rocks are widely distributed in the Zhongdian area. Two northwest–southeast trends of intrusive rock belts are identified in Hongshan anticline. The east belt spreads from Wodicuo (northwest) to Pulang (southeast). The west belt includes Gaochiping, Lannitang, Xuejiping, and Chundu intrusive rocks. K–Ar dating of biotite from the Langdu intrusions yields ages of 216.93 ± 4.3 Ma (Zeng et al., 2004). Pulang intrusions have yielded two K–Ar isotopic ages from 216.0 ± 1 to 221.5 ± 2.0 Ma, and a U–Pb isochron age of

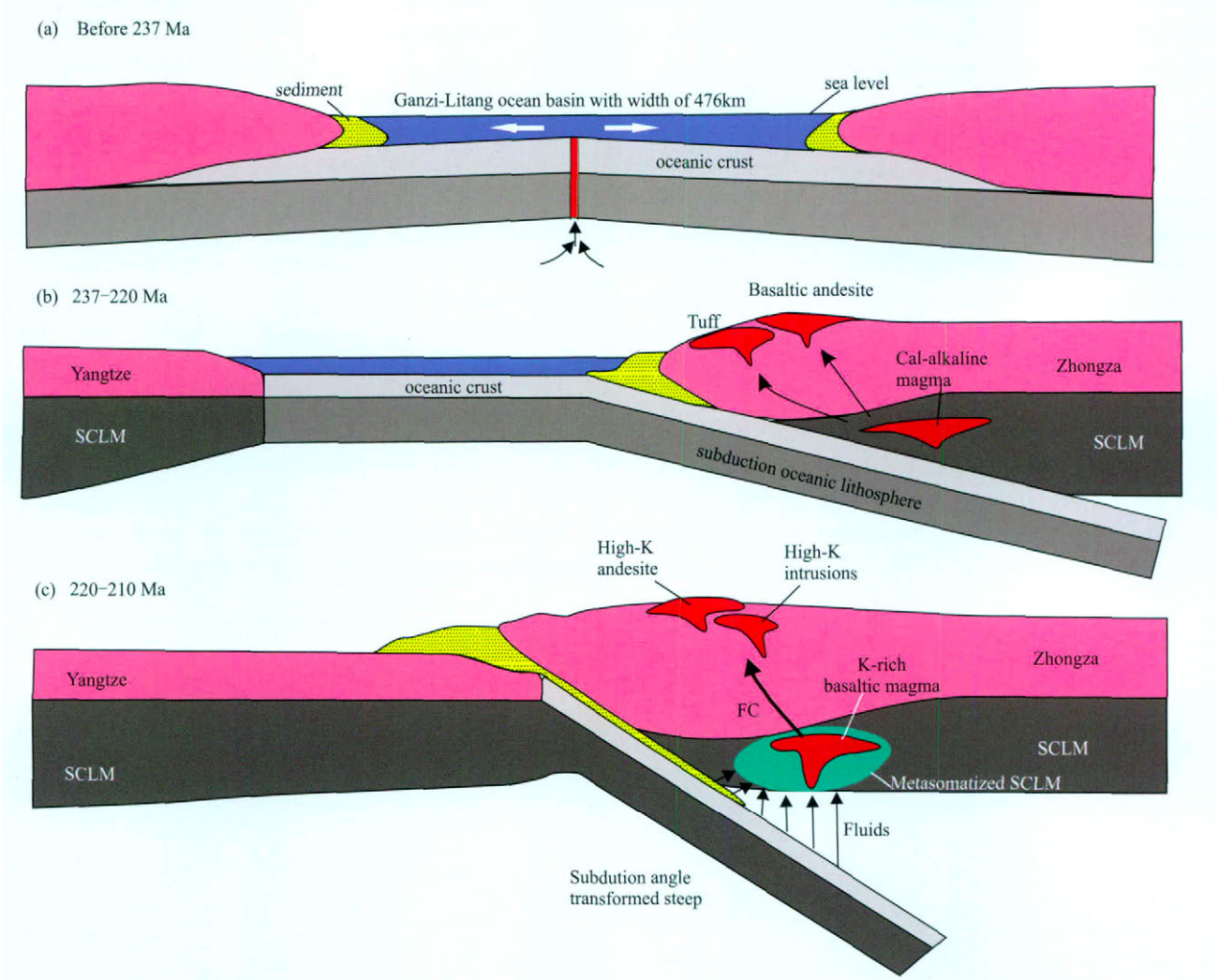

Fig. 12. Tectonic evolution model of the Zhangdian island arc. SCLM=subcontinental lithospheric mantle, FC=factional crystallization.

226–228 Ma (Wang et al., 2008). On the other hand, zircon SHRIMP dating for the Xuejiping, Songruo, and Chundu intrusive rocks have yielded ages of 215.3 ± 2.3 Ma (Lin et al., 2006), 220.9 ± 3.5 Ma (Leng et al., 2009), and 212–218 Ma (Yang et al., 2011), respectively. Reid et al. (2007) dated Daocheng and Changtai granites (length ~350 km and width ~70 km) to yield zircon U–Pb isochron ages of 215 and 218 Ma, respectively. The presence of these high–K calc–alkaline igneous rocks in the Zhongdian area and granites in the northwestern region in large scales suggests that the closure of the Garzê–Litang ocean basin resulted in the Late Triassic (Fig. 12c; Hou et al., 2001).

In summary, the most important magmatic event occurred in Yidun island arc over about 210–220 Ma. High–K calc–alkaline and shoshonitic series rocks are considered to be typical continental collision rocks (continent–arc collision or continent–continent collision; Deng et al., 2004). Previous studies assumed that high–K intrusive rocks in the Zhongdian area and granite emplacement in the Changtai and Daocheng island arcs were the products of Garzê–Litang ocean subduction (Yang et al., 2002; Zeng et al., 2004; Wang et al., 2008) and late subduction (Hou et al., 2003) stages, respectively. In our view, the large–scale magmatic activity cannot be triggered by the subduction setting only; on the contrary, it may reflect that the arc–continent collision has occurred.

Acknowledgments

The author wishes to thank C.Z. Yang (Branch of Mineral Resources Investigation, Yunnan Geological Survey, China) for the helpful discussions on the geology of the Zhongdian area and for providing information on the Langdu deposit. This study was jointly supported by the National Science Foundation of China (NSFC) project (41203039) and the innovation team of ore–forming dynamics and prediction of concealed deposits, KMUST (2008).

Manuscript received May 16, 2012
accepted Oct. 15, 2012
edited by Liu Lian

References

Acef, K., Liégeois, J., Ouabadi, A., and Latouche, L., 2003. The Anfeg post–collisional Pan–African high–K calc–alkaline batholith (Central Hoggar, Algeria), result of the LATEA microcontinent metacratonization. *J. Afr. Earth Sci.*, 37(3): 295–311.

Ayers, J., 1998. Trace element modeling of aqueous fluid–peridotite interaction in the mantle wedge of subduction zones. *Contrib. Mineral Petrol.*, 132: 390–404.

Benito, R., Lopez, R.J., Cebriá, J.M., Hertogen, J., Doblas, M., Oyarzun, R., and Demaiffe, D., 1999. Sr and O isotope constraints on source and crustal contamination in the high–K calc–alkaline and shoshonitic Neogene volcanic rocks of SE Spain. *Lithos*, 46(4): 773–804.

Boztug, D., Arehart, G., Platevoet, B., Harlavan, Y., and Bonin, B., 2007. High–K, calc–alkaline I–type granitoids from the composite Yozgat batholith generated in a post–collisional setting following continent–oceanic island arc collision in central Anatolia, Turkey. *Miner. Petrol.*, 91(3): 191–223.

Calvin, F.M., McDowell, S.M., and Mapes, R.W., 2003. Hot and cold granites? Implication of zircon saturation temperatures and preservation of inheritance. *Geology*, 31(6): 529–532.

Cao Dianhua, Wang Anjian, Xiu Qunye, Yang Yueqing and Li Ruiping, 2007. Geochemical characteristics of bengge syenites in the zhongdian area Yunnan province and its geological significance. *Acta Geological Sinica*, 81: 995–1003 (in Chinese with English abstract).

Conticellia, S., and Peccerillo, A., 1992. Petrology and geochemistry of potassic and ultrapotassic volcanism in central Italy: petrogenesis and inferences on the evolution of the mantle sources. *Lithos*, 28(3–6): 221–240.

Deng Jinfu, Luo Zhaohua, Su Guoshang, Mo Xuanxue, Yu Binsong and Lai Xingyun, 2004. *Genesis, tectonic setting and mineralization*, Beijing, Geological Publishing House, 38 (in Chinese with English abstract).

Evans, O.C., and Hanson, G.N., 1993. Accessory–mineral fraction of rare earth element abundance in granitoid rocks. *Chem. Geol.*, 110: 69–93.

Féménias, O., Berza, T., Tatu, M., Diot, H., and Demaiffe, D., 2008. Nature and significance of a Cambro–Ordovician high–K, calc–alkaline sub–volcanic suite: the late–to post–orogenic Motru Dyke Swarm (Southern Carpathians, Romania). *Int. J. Earth Sci.*, 97(3): 479–496.

Foley, S.F., 1992. Potassic and ultrapotassic magmas and their origin. *Lithos*, 28: 181–185.

Hanson, J.N., 1978.The application of trace–elements to the petrogenesis of igneouse rocks of granitic composition. *Earth Planet. Sci. Lett.*, 38: 26–43.

Hart, S.R., 1984.The DUPAL anomaly: A large scale isotopic mantle anomaly in the Southern Hemisphere. *Nature*, 309: 753–757.

Hart, S.R., 1988. Heterogeneous mantle domins, genesis and mixing chronologies. *Earth Planet. Sci. Lett.*, 90: 73–276.

Hou Zengqian, Yang Yueqing, Qu Xiaoming, Huang Dianhao, Lv Qingtian, Tang Shaohua, Yu Jinjie, Wang Haiping and Zhao Jinhua, 2001. Collision–orogenic processes of the Yindun arc in the sanjiang region: record of granites. *Acta Geologica Sinica*, 75: 485–497 (in Chinese with English abstract).

Hou Zengqian, Yang Yueqing, Qu Xiaoming, Huang Dianhao and Lv Qingtian, 2004. Tectonic evolution and mineralization systems of the Yidun arc orogen in sanjiang region, china. *Acta Geologica Sinica*, 78: 109–120 (in Chinese with English abstract).

Hou Zengqian, Yang Yueqing, Wang Haiping, Qu Xiaoming, Lv Qingtian, Huang Dianhao, Wu Xuanzhi, Yu Jinjie, Tang Shaohua and Zhao Jinhua, 2003. *Orogenic and mineralization system in Yindun island arc*. Beijing, Geological Publishing House, 1–345 (in Chinese).

Lan, C.Y., Lee, T., and Wang, Lee. C., 1990. The Rb–Sr isotopic

record in Taiwan gneisses and its tectonic implication. *Tectonophysics*, 183:129–143.

Leng Chengbiao, 2009. *Ore deposit geochemistry and regional geological setting of Xuejiping porphyry copper deposit, Northwest Yunnan, China*. Guiyang: State Key Laboratory of Ore Geochemistry of CAS (Ph. D thesis): 89–100 (in Chinese with English abstract).

Li Dapeng, Luo Zhaohua, Liu Jiaqi, Chen Yuelong and Jin Ye, 2012. Magma origin and evolution of tengchong Cenozoic volcanic rocks from west Yunnan, China: evidence from whole rock geochemistry and Nd–Sr–Pb isotopes. *Acta Geologica Sinica* (English edition), 86(4): 867–878.

Li Xianhua, Zhou Hanwen, Liu Ying, Li Jiyu, Chen Zhenghong, Yu Jinsheng and Gui Xuntang, 2001.Mesozoic shoshonitic intrusives in the Yangchun basin,western Guangdong, and their tectonic significance:II. Trace elements and Sr–Nd isotopes. *Geochimica*, 30: 56–65 (in Chinese with English abstract).

Li Xianhua, Zhou Hanwen, Liu Ying, Li Jiyu, Chen Zhenghong, Yu Jinsheng and Gui Xuntang, 2000. Mesozoic shoshonitic intrusives in the Yangchun basin, western Guangdong, and their tectonic significance: I. Petrology and isotope geochronology. *Geochimica*, 29: 513–521 (in Chinese with English abstract).

Lin Qingcha, Xia Bin and Zhang Yuquan, 2006. Zircon SHRIMP U–Pb dating of the syn–collisional Xuejiping quartz diorite porphyrite in Zhongdian, Yunnan, China, and its geological implications. *Geological Bulletin of China*, 25: 133–137 (in Chinese with English abstract).

Litvinovsky, B.A., Steele, I.M., and Wickham, S.M., 2000. Silicic magma formation in overthickened crust: melting of charnockite and leucogranite at 15, 20 and 25 kbar. *J. Petrol.,* 41(5): 717–737.

Middlemost, E.A., 1994. Naming materials in the magama/ igneous rock system. *Earth Sci. Rev.*, 37: 215–224.

Mo Xuanxue, Lu Fengxiang, Shen Shangyue, Zhu Qinwen, Hou Zengqian, Yang Kaihui, Deng Jinfu, Liu Xiangpin and He Changlin, 1993. *Volcanism and mineralization of Sanjiang Tethyan*. Beijing, Geological Publishing House, 1–267 (in Chinese with English abstract).

Morrison. G., 1980. Characteristics and tectonic setting of the shoshonite rock association. *Lithos*, 13(1): 97–108.

Nelson, D.R., McCulloch, M.T., and Sun, S.S., 1986. The origins of ultrapotassic rocks as inferred from Sr, Nd and Pb isotopes. *Geochim. Cosmochim. Ac.*, 50(2): 231–245.

Neves, S., Mariano ,G., Guimaraes, I.P., da Silva Filho, A.F., and Melo, S.C., 2000. Intralithospheric differentiation and crustal growth: evidence from the Borborema province, northeastern Brazil. *Geology,* 28(6): 519–522.

Njanko, T., Nédélec, A., and Affaton, P., 2006. Synkinematic high–K calc–alkaline plutons associated with the Pan–African Central Cameroon shear zone (W–Tibati area): Petrology and geodynamic significance. *J. Afr. Earth Sci.*, 44(4–5): 494–510.

Palacz, Z.N., and Saunders, A.D., 1986. Coupled trace element and isotope enrichment in the Cook–Austeal–Samoa island, southwest Pacific. *Earth Planet. Sci. Lett.*, 79: 270–280.

Plank, T., 2005. Constraints from thorium/lanthanum on sediment recycling at subduction zones and the evolution of the continents. *J. Petrol.*, 46: 921–944.

Putirka, K., and Busby, C., 2007. The tectonic significance of high–K_2O volcanism in the Sierra Nevada, California. *Geology*, 35(10): 923.

Qi Liang, Hu Jing and Gregoire, D.C., 2000. Determinition of trace elements in granites by inductively coupled plasma mass spectrometry. *Talanta*, 51: 507–513.

Reid, A., Wilson, C.J.L., Shun, L., and Belousovac, E., 2007. Mesozoic plutons of the Yidun Arc, SW China: U/Pb geochronology and Hf isotopic signature. Ore Geol. Rev., 31 (1–4): 88–106.

Roberts, M.P., and Clemens, J.D., 1993. Origin of high–potassium, calc–alkaline, I–type granitoids. *Geology*, 21: 825–828.

Rottura, A., Bargossi, G.M., Caggianelli, A., Del Moroc, A., Visonàd, D., and Trannea, C.A., 1998. Origin and significance of the Permian high–K calc–alkaline magmatism in the central –eastern Southern Alps, Italy. *Lithos*, 45(1–4): 329–348.

Sun, S.S., and McDonough, W.F., 1989. Chemical and isotopic systematics of oceanic basalts: implications for mantle composition and processes. *Geological Society, London, Special Publications*, 42: 313–345.

Tatsumi, Y., and Kogiso, T., 1997. Trace element transport during dehydration processes in the subducted oceanic crust: 2. Origin of chemical and physical characteristics in arc magmatism. *Earth Planet. Sci. Lett.*, 148: 207–221.

Wan Tianfeng and Zhu Hong, 2011. Chinese continental blocks in global paleocontinental reconstruction during paleozoic and mesozoic. *Acta Geologica Sinica* (English edition), 85(3): 581 –597.

Wang, K.L., Chung, S.L., O'Reilly, S., Sun, S.S., Shinjo, R., and Chen, C.H., 2004. Geochemical constraints for the genesis of post–collisional magmatism and the geodynamic evolution of the Northern Taiwan Region. *J. Petrol.*, 45: 975–1011.

Wang Shouxu, 2008. *Ore geochemistry of Pulang porphyry copper deposit, Yunnan Province, China*. Guiyang: State Key Laboratory of Ore Geochemistry of CAS, (Ph. D thesis): 89–100 (in Chinese with English abstract).

Weaver, B.L., Wod, D.A., Tarney. J., and Joron, J.L., 1986. Role of the subducted sediment in the genesis of ocean–island basalts: Geochemical evidence from South Atlantic Ocean islands. *Geology,* 14: 275–278.

Xiao Long, Xu Yigang, Xu Jifeng, He Bin and Pirajno, F., 2004. Chemostratigraphy of flood basalts in the Garzê–Litang region and Zongza block: implications for Western extension of the Emeishan large igneous province, SW China. *Acta Geologica Sinica* (English edition). 78(1): 61–67.

Xu Jifeng and Castillob, P.R., 2004. Geochemical and Nd–Pb isotopic characteristics of the Tethyan asthenosphere: implications for the origin of the Indian Ocean. *Tectonophysics*, 393: 9–27.

Yang Yueqing, Hou Zengqian, Huang Dianhao and Qu Xiaoming, 2002. Collision orogenic process and magmatic metallogenic system in Zhongdian arc. *Acta Geoscience Sinica*, 23: 17–24 (in Chinese with English abstract).

Zeng Pusheng, Wang Haiping, Mo Xuanxue, Yu Xuehui, Li Wenchang, Li Tigang, Li Hong and Yang Chaozhi, 2004. Tectonic setting and prospects of porphyry copper deposits in Zhongdian island arc belt. *Acta Geoscience Sinica*, 25: 535–540 (in Chinese with English abstract).

Zindler, A., and Hart, S.R., 1986. Chemical geodynamics. A*nn. Rev. Earth Planet. Sci. Lett.*, 14: 493–571.